An Acad Bras Cienc (2024) 96(Suppl. 1): e20240040 DOI 10.1590/0001-3765202420240040
Anais da Academia Brasileira de Ciências | *Annals of the Brazilian Academy of Sciences*
Printed ISSN 0001-3765 I Online ISSN 1678-2690
www.scielo.br/aabc | www.fb.com/aabcjournal

CHEMICAL SCIENCES

Analysis of Tribology Properties of Trimethylolpropane-based Lubricant by Molecular Dynamics

CAMILA B. SOUZA, RENE FRANCISCO B. GONÇALVES & JOSÉ ATÍLIO F.F. ROCCO

Abstract: Currently, it is crucial for the lubricant formulation industry to explore cost-effective and environmentally friendly methodologies for analyzing the tribological properties of engine aviation lubricants under high-temperature and high-pressure operating conditions. This study demonstrates the feasibility of employing molecular dynamic simulations to gain essential insights into the evolution of the tribological properties of lubricants during operation. A three-layer molecular model was devised, comprising nickel aluminide molecules in the top and bottom layers, and polyol ester in the core. The impact of sliding velocities ranging from 20 km/h to 100 km/h was investigated under varying temperature and pressure conditions. Concentration, temperature and velocity profiles, radial distribution function, mean square displacement, and friction coefficient were calculated and analyzed in detail. Notably, the highest friction coefficients – ranging from 2.5 to 0.75 - were observed at the lowest temperature and pressure conditions tested. Conversely, other sections of the gas turbine exhibited substantially lower friction coefficients – ranging from 0 to 0.01.Simulations demonstrate that increasing pressure and temperature reduce polymer chain mobility, leading to stronger internal interactions within the lubricant. Consequently, lubricant adsorption onto metal surfaces decreases. Furthermore, the lubricant performs exceptionally well when its molecules encounter higher velocities and temperatures. Based on the results obtained, the research demonstrates that the presented technique provides both quantitative and qualitative tribological information essential for understanding a system molecular behavior, serving as a guiding framework for researchers in the field.

Key words: Lubricant, tribology, trimethylolpropane, aviation engine, dynamic molecular, materials studio.

INTRODUCTION

The progress of aircraft propulsion is significant, making it essential for aviation as a mode of human locomotion (El-Sayed 2017). Nowadays, gas turbines are the most efficient engines for generating thrust in aircraft (Petrescu et al. 2017). Simply put, these turbines operate by capturing, compressing, and reacting air with fuel. This process releases energy to turn turbines, providing the thrust necessary for aircraft propulsion. The entire operation subjects the engines to extreme conditions - high temperature and pressures in oxidative and catalytic environments (El-Sayed 2017, Meetham 1981, Wu et al. 2017).

Alongside the progress in aircraft propulsion, the development of advanced lubricants has become intricately linked with the evolution of materials used in engine construction. Advanced lubricants are formulated to complement the properties of modern materials, such as carbon composites, ceramic matrix composites, and hightemperature alloys, which are increasingly employed in engine components (Basheer 2020). These materials demand lubricants that can withstand extreme temperatures, pressures, and mechanical stresses while providing effective lubrication and protection against wear and corrosion (Dekoulis 2019, Siouris & Wilson 2010, Sun & Du 2019, Wakiru et al. 2019). Moreover, the integration of nanomaterials into lubricant formulations has enabled tailored lubrication solutions that optimize the performance and longevity of advanced engine materials (Ali et al. 2019). By synergizing with these advanced materials, lubricants play a crucial role in enhancing the efficiency, reliability, and environmental sustainability of aircraft propulsion systems. The ongoing advancement of both lubricant and material technologies promises further innovations in aviation, driving towards more efficient and environmentally friendly aircraft operations.

Currently, the most commonly used classes of lubricants in aviation are polyolefins, diesters and polyol esters due to their chemical structure being more resistant to thermal degradation (Nagendramma & Kaul 2012). Among these options, polyol esters stands out due to their superior thermo-oxidative stability, and consequently, better performance (Raof et al. 2019). Additionally, it is important to emphasize that any lubricant will change its physical and chemical properties during use due to the harsh operational environment (Siouris et al. 2013). Thus, it is evident that lubricant quality directly influences turbine operation (Srivastava et al. 2021). This underscores the importance of investing in the field of lubricant formulation - both in creating new lubricants and optimizing existing ones (Sun & Du 2019, Wakiru et al. 2019).

A central issue in lubricants research and development is understanding its behavior under real-use conditions. Essentially, the technology used for analyzing this aspect comprises practical tests. The main tests used are static test bed, engine oil under in-service conditions and laboratory-based short-duration oxidation testing (Siouris et al. 2013). The static test bed involves removing oil during engine development or certification activities. Its disadvantages include subjecting the oil to higher stress than in real conditions and the high cost involved. The engine under inservice conditions test is the most accurate way to determine lubricant behavior but is rarely performed due to resistance from operators who see it as an interruption of revenue-generating operations. Consequently, laboratory-based short-duration oxidation testing has been extensively utilized, although it subjects lubricants to more extreme conditions, distorting the data obtained from real-life scenarios (Siouris et al. 2013).

Usually, the main properties evaluated in a lubricant are viscosity and density, as they directly influence the lubricant's hydrodynamics (Lin & Kedzierski 2020). Additionally, the friction process presents important parameters in the tribology study, known as wear rate and friction coefficient. Other relevant information includes interface friction, as it influences shear deformation (Cui et al. 2021). In the literature, these aspects are frequently obtained by molecular dynamics (MD). Pan et al. (2021) used MD to study the boundary lubrication behaviors of squalene during shearing at different pressures and temperatures. It indicated that the nanostructure surface has a significant effect on the thickness and delamination of the lubricating film but little effect on its velocity distribution. Additionally, the film helps to reduce the coefficient of friction of the system. Guo

et al. (2021) investigated the friction in rubber-tire pavement systems under different velocities and temperatures using MD. The results showed that different system combinations present different friction performances. However, it was unanimous that the changes in longitudinal stress during the attrition process influence the coefficient of friction. Cui et al. (2021) analyzed the mechanical and tribological effects of different reinforcements added to elastomers using molecular dynamics. They found that amide-functionalized CNTs presented the best reinforcement efficiency. They also studied interfacial regions through temperature and relative concentration. Li et al. (2016) investigated changes in the tribological properties of a nitrile-butadiene rubber reinforced with carbon nanotubes. It showed that reinforcement affects the friction interface and improves the elastomer's tribological properties. In this case, the interface exhibited a decrease in the concentration of atoms, the temperature peak, the speed of atom movement, and the average cohesive energy. Zojaji et al. (2021) presented the influence of shear rate and temperature on fluids using nonequilibrium molecular dynamics simulations. The authors used radial distribution function (RDF) to show the relationship between the atomic phase transition and the shear thickening phenomena observed. Finally, the rheological results showed that the DREIDING and Universal force fields can simulate fluids and estimate their rheological behavior. Hu et al. (2021) investigated the mobility and activity of phenolic antioxidants in oil of trimethylolpropane trioleate (TMPTO), as well as the oxygen permeability in this compound. The results of minimal squared distance (MSD) were important to evaluate the mobility of antioxidants.Experimental data showed that antioxidant molecules with higher molecular weights and longer phenolic hydroxyl groups have better oxidative resistance, consistent with the simulations performed.

In this context, this report presents a low cost and reliable simulation methodology to analyze the behavior of lubricants under turbine aircrafts conditions. Computer simulation is an environmentally friendly option because it reduces experimental cost and avoids wasting laboratory resources (Srivastava et al. 2021). This research proposes the use of molecular dynamics (MD), an underexplored method for this purpose. MD simulation acts as a bridge between microscopic and time scales, allowing testing theories without necessarily performing laboratory experiments (Haile 1992, Srivastava et al. 2021). Molecular dynamics is suitable for tribological studies, as time-dependent processes and transport coefficients are more easily obtained through this means (Ewen et al. 2018). A commercial software that stands out for its effectiveness in conducting molecular dynamics studies is Materials Studio. Its user-friendly interface simplifies and makes simulations more accessible. Most studies in the field of tribology using Materials Studio examine the tribological behavior of materials (Huang 2012), changes in material properties when adding reinforcement or additives (Chawla & Sharma 2018, Hu et al. 2021, Li et al. 2016, Liu et al. 2021, Cui et al. 2021, Yin et al. 2022), or how different treatments on these reinforcements impact these properties (Qi et al. 2023, Talapatra & Datta 2023). Some studies evaluate the effects of speed, pressure, and temperature on the friction process (Guo et al. 2021, Zeng & Chen 2018, Zojaji et al. 2021) and the performance of lubricants on different surfaces (Ta et al. 2015). However, no studies were found evaluating lubricants under extreme conditions of temperature and pressure simultaneously.

METHODOLOGY

All molecular dynamics (MD) simulations were conducted using Materials Studio (MS) 7.0 software from Accelyrs, USA. The simulation cells comprised nickel aluminide ($NiAl3$) and Trimethylolpropanetriheptanoate ester ($C27H50O6$). Nickel aluminide was selected due to its widespread use in aircraft turbines, while the lubricant was chosen for its remarkable performance under extreme conditions, maintaining its tribological properties despite mechanical strain in high-pressure and high-temperature environments (Bakan et al. 2020, El-Magly et al. 2018). The simulations utilized the Universal force field, an all-atom type, with parameterization for all atoms with atomic numbers lower than 103 (Jaillet et al. 2017). The broad inclusiveness of this force field made it ideal for the diverse atoms in our system. The Universal force field can be described by Equation (1) (Rappe et al. 1992):

$$E_{(total)} = \frac{1}{2}K_{ij}(r - r_{ij})^2 + K_{ijk}\sum_{n=0}^{m} C_n \cos(n\theta) + K_{ijk}\sum_{n=0}^{m} C_n \cos(n\phi_{ijkl}) + K_{ijkl}\sum_{n=0}^{m} C_0 + C_1 \cos + \omega_{ijkl} + C_2 \cos\omega_{ijkl} + D_{ij} - 2(\frac{X_{ij}}{X})^6 + (\frac{X_{ij}}{X})^{12} + 332,0637(\frac{Q_i Q_j}{\epsilon R_{ij}}). \quad (1)$$

where Kij is a force constant with units of (kcal/mol)/Å2, rij is the standard or natural bond length in Å and Θ is the bond angle.

The pure NiAl3 atoms layer was modeled using triclinic crystal with dimensions of 13.00 x 14.70 x 9.60 Å. The lubricant cell was constructed with 113 molecules in a 44.95 x 44.95 x 44.95 Å amorphous cell. To investigate the tribological properties of the $NiAl_3$ and ($C27H50O6$) system, a three-layer model with dimensions of 45.00 x 45.00 x 84.20 Å was created. In this model, the lubricant is confined between two metal surfaces, with a 20 Å vacuum layer above the upper wall to avoid interaction through mirror image in the z direction. Figure 1 shows the three-dimensional model of the system.

Four simulation steps were performed on the three-dimensional model using the Forcite module. Van der Waals forces and electrostatic interactions were calculated using the atom-based summation method with a cutoff distance of 22.5 Å - this cutoff distance allows capturing significant interactions within the system without including undesired interactions due to the periodicity of the box. The atom-based summation method was selected due to its computational efficiency and ability to handle moderately sized molecular systems. This approach allows the calculation of interactions among all pairs of atoms in the system, ensuring an accurate representation of intermolecular interactions without incurring prohibitive computational costs. Initially, the lowest energy conformation was obtained through geometry optimization using the conjugate gradient algorithm - due to its computational efficiency, numerical stability, and adaptation to complex molecular systems - with an energy convergence tolerance of 0.01 kcal/mol and a force convergence tolerance of 0.5 kcal/mol/Å. The upper and lower $NiAl_3$ layers were kept fixed during this optimization.

Subsequent simulations used this optimized conformation. A five-cycle annealing process was conducted from 300 K to 500 K over 50 ps in an NVT ensemble, with a 1 fs timestep. Temperature control was achieved using a Berendsen thermostat due to its efficiency, simplicity, and adaptation to systems containing polymers and metal. Its numerical stability and validation in previous studies also contributed to its selection. After each annealing cycle, the structure was re-optimized. Next, the

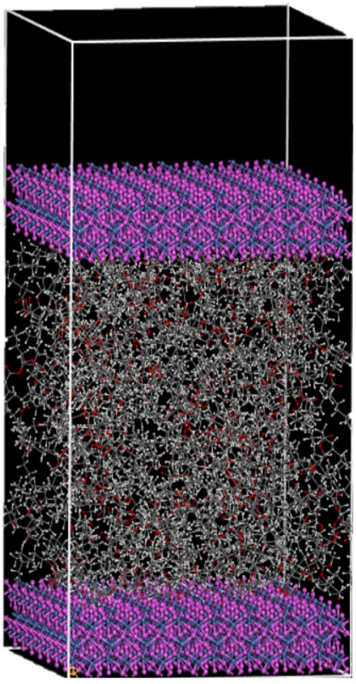

Figure 1. Three-dimensional model of the system.

models were dynamically equilibrated in an NPT ensemble at 298 K using the Berendsen thermostat and 1 atm using the Andersen barostat. This type of barostat was chosen due to its efficiency in pressure control, simple implementation, and adaptation to different experimental conditions. The timestep was set to 1 fs with a 200 ps relaxation period per cycle, continuing until total energy and temperature convergence.

Finally, shear velocity was applied to both walls of the model. It was applied using confined shear – it refers to the deformation experienced by a material when subjected to shear forces within a constrained environment. To simulate confined shear, it is allowed the walls of the cell to move in response to the applied shear forces. This movement of the walls effectively constrained the material, leading to the observed confined shear behavior and how the material responded to these to shear forces over time forces. The process was achieved by moving it at varying velocity rates (0.06, 0.11, 0.17, 0.22, 0.28 Å/ps) over 400 ps with a 1 fs timestep under NPT conditions. Temperatures and pressure parameters were based on a singlespoon type tubojet engine model (El-Sayed 2017).

Three regions of the engine were chosen: intake duct (Temperature = 276.3 K; Pressure = 0.61 atm), combustion chamber (Temperature = 1200 K; Pressure = 4.69 atm) and the outlet nozzle (Temperature = 848.2 K; Pressure = 1.03 atm). Lubricant was also simulated at environmental conditions (Temperature = 298.15 K; Pressure = 1 atm) for comparison purposes. The trajectory of atoms and forces generated in the sliding direction were recorded for calculating tribological properties, – including the coefficient of friction and viscosity, as well as the interfacial region of metal and lubricant as velocity profile, concentration profile, temperature profile, mean square displacement (MSD), and radial distribution function (RDF). The MSD for all molecular dynamics runs was calculated every 200 timesteps using the centroid form. In statistical mechanics, the radial distribution function (RDF) of a molecular system depicts how density changes with distance from a reference point (Su et al. 2020). In this study, the

RDF is calculated for the centroids of all lubricant molecules, providing a measure of the probability of locating a molecule at a distance r from the specified reference point.The selected molecules for both MSD and RDF calculations were the lubricant $C_{27}H_{50}O_6$, i.e. the liquid layer of the system (for this calculation, the software has computed the radial distribution function for all pairs of atoms in the fluid set). Figure 2 provides a flowchart visualizing the steps of the methodology used.

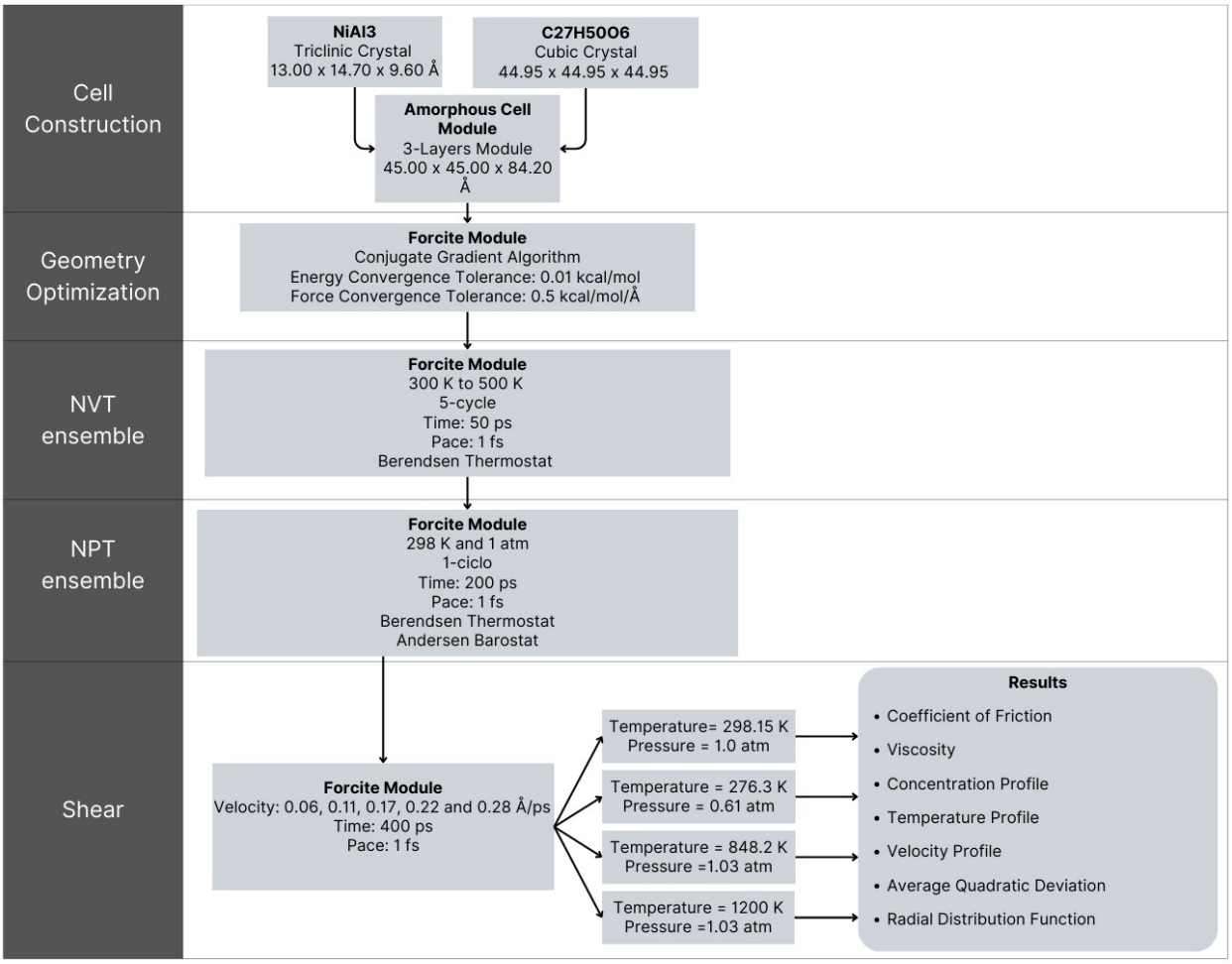

Figure 2. Flowchart of the methodology used in the article.

RESULTS AND DISCUSSION

For this study, we investigated the variability of lubricant under different shear sliding velocities. The velocities chosen were 20 km/h, 40 km/h, 60 km/h, 80 km/h and 100 km/h, which corresponded at the atomistic level to 0.06 Å/ps, 0.11 Å/ps, 0.17 Å/ps, 0.22 Å/ps and 0.28 Å/ps, respectively. These velocities were applied to the top and bottom wall layers during the confined shear process. In all results, curves (A), (C), and (D) of Fig. 2 pertain to the lubricant in different areas of a turbine, while curve (B) represents the lubricant at ambient temperature and pressure.

Relative Concentration

Figure 3 presents the relative concentration (RC) profile of the lubricant under different velocities in various turbine regions. RC represents the density of particles in a specific region of the system. This information is important for analyzing the distribution of lubricant density and assessing whether the lubricant is functioning efficiently. The value of RC can be obtained using Equation 2 (Cui et al. 2021). Additionally, it's worth noting that relative concentration is dimensionless, meaning an RC value of 2 indicates that there are twice as many molecules in a particular region, assuming all molecules were uniformly distributed throughout the system.

$$RC = \frac{R_{layer}}{R_{system}}. \tag{2}$$

Where: Rlayer represents the ratio of the number of atoms in the layer to the volume of the layer; Rsystem represents the ratio of the total number of atoms in the system to the volume of the system.

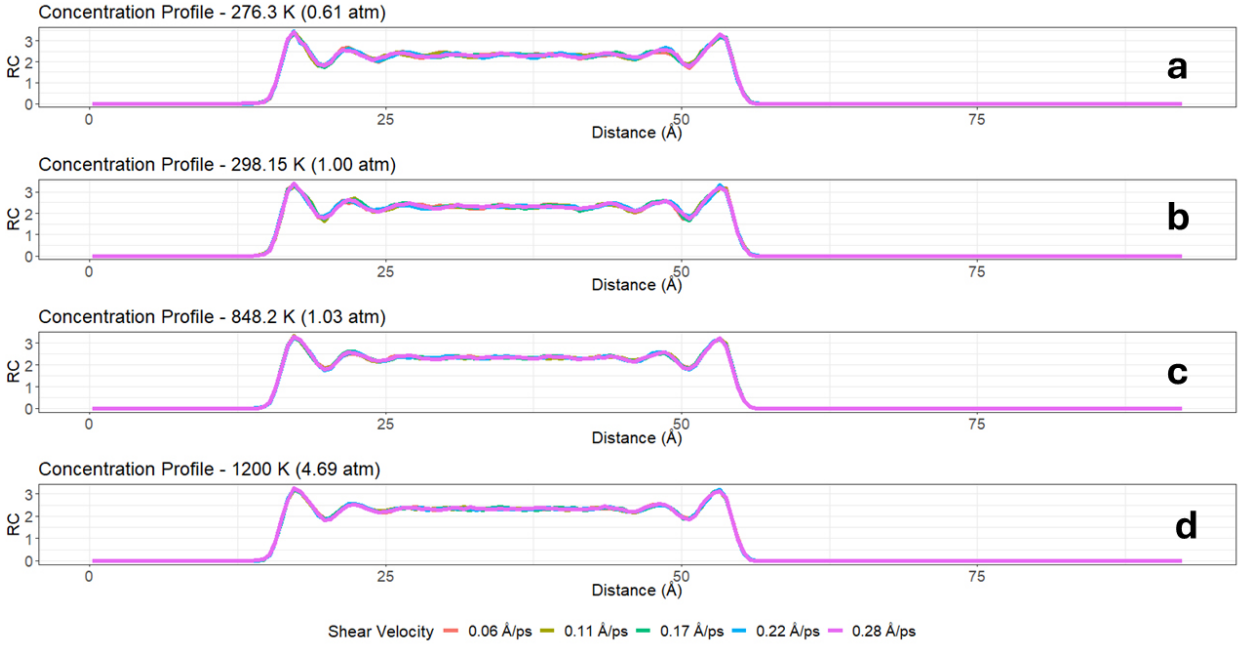

Figure 3. Curves illustrating the relative concentration profile of the lubricant under varying shear velocities in different settings: (a) Intake, (b) Ambient Conditions, (c) Outlet Nozzle, and (d) Combustion Chamber.

All the graphs consistently show peaks at 15 Å and 60 Å, indicating the highest values. In the innermost region of the system, between these peaks, the curve is nearly linear with some oscillations in the regions near the interfacial area. This curve shape suggests a higher atomic concentration of lubricant in the interfacial region, attributed to the adsorption between the lubricant and the metal (Zhang et al. 2020). Tipically, a strong affinity between the lubricant and the metal results in higher adsorption, which can be detrimental as it retains many lubricant molecules in this region, leaving fewer molecules available to participate in the shearing/sliding process performed by the lubricant, which reduces friction.

Furthermore, diminished mobility of molecules with high molecular mass can negatively affect their tribological effectiveness in several ways. Firstly, it impairs the formation of a protective lubricating film due to limitations in their ability to migrate and rearrange. Secondly, it diminishes load-carrying capacity by potentially resulting in inadequate viscosity enhancement, leading to a thinner lubricating film, increased friction, and wear. Lastly, it hampers the redistribution of lubricant on surfaces by inhibiting efficient flow and spreading, which can result in localized lubricant depletion and heightened metal-to-metal contact, thereby accelerating wear and compromising overall efficacy. Therefore, ensuring adequate mobility of these molecules is essential to maintain optimal lubricant performance and protect components from excessive friction and wear. Thus, it's desirable for a lubricant to have a curve with more intensity in the interface region. The differences between the curves in different environments is subtle, with a higher presence of lubricant observed inside the cell at high temperatures and pressures compared to the interface with the metal. This indicates that the environment influences the lubricant's concentration gradient in use, likely due to the restricted movement in locations with lower temperature and pressure.

Temperature

Figure 4 shows the temperature in the longitudinal profile of the lubricant during the friction process under the influence of different velocities in various regions of a turbine. As depicted in Figure 4, the temperatures at the frictional interfaces reach their maximum levels at 10 Å and 60 Å, due to the shear deformation and adhesive friction generated during the frictional process (Cui et al. 2021). Any of the plots shows that the internal temperature of the lubricant remained relatively stable for every shear rate, with minimal temperature fluctuations. In all the graphs, it is evident that both the lubricant's temperature at the boundaries and its temperature within the system are higher than that of the environment condition, indicating that, in addition to reaching thermal equilibrium with the engine region, the lubricant absorbs heat from the frictional process, contributing to cooling the system. Furthermore, upon analyzing each graph individually, it becomes apparent that varying the applied shear rate leads to a modification in the lubricant's temperature profile during friction. In this case, higher shear rates (0.17, 0.22, 0.28 Å/ps) result in higher values in the interface region. This behavior is expected as higher velocities in this region lead to increased shear deformation and adhesive friction.

Velocity

Figure 5 presents the velocity profile of the lubricant during the friction process under different velocities in various turbine regions. It is evident in all the curves that there are peaks of velocity within the friction areas, specifically at distances of 10 Å and 60 Å. This velocity pertains to the relative motion of the lubricant with respect to the substrate (Xu et al. 2021). Both negative and positive velocity values are observed due to the adopted reference, as the lubricant moves in opposite directions relative to the substrates. It should be noted that the higher the peak of velocity, the greater the lubricant's velocity in the contact region with the metal, resulting in better tribological performance. It is noticeable that, as the temperature and pressure of the environment increase, the lubricant's velocity also increases. This is due to the ambient temperature generating an increase in the internal energy of the material, which enhances its performance under these conditions (Yin et al.

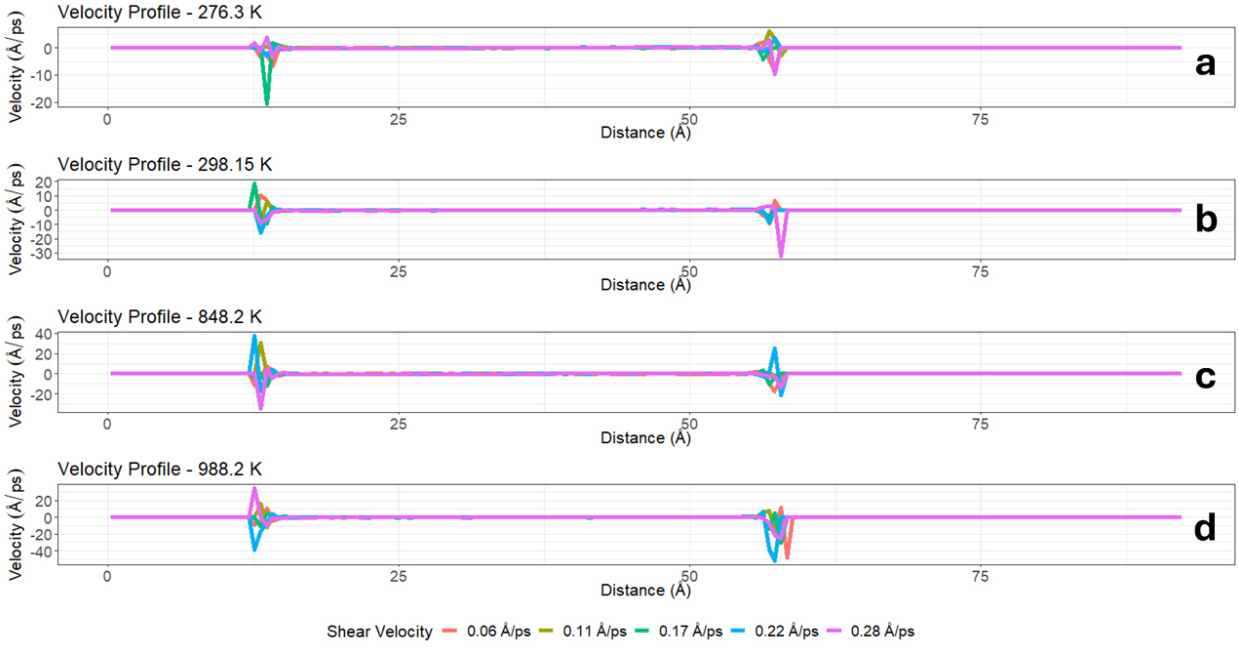

Figure 4. Curves illustrating the temperature profile of the lubricant under varying shear velocities in different settings: (a) Intake, (b) Ambient Conditions, (c) Outlet Nozzle, and (d) Combustion Chamber.

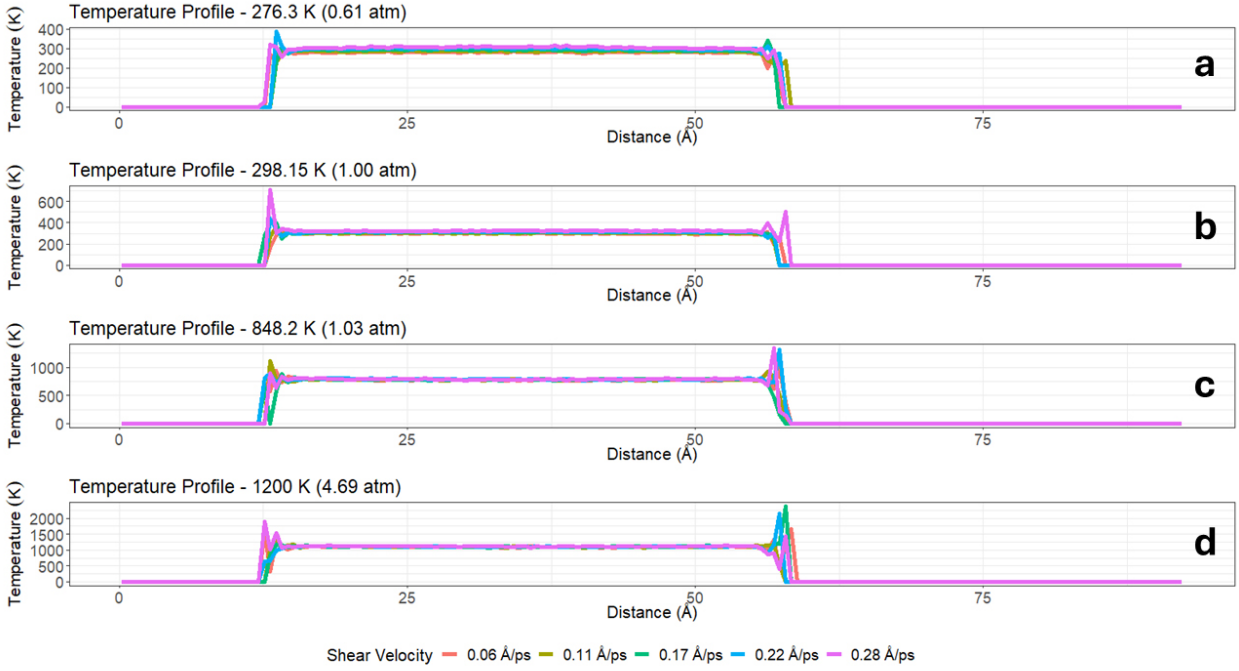

Figure 5. Curves illustrating velocity profile of the lubricant under varying shear velocities in different settings: (a) Intake, (b) Ambient Conditions, (c) Outlet Nozzle, and (d) Combustion Chamber.

2022). Additionally, the applied shear velocity affects the behavior of the lubricant's relative motion, but without a specific pattern, indicating that a high shear velocity does not necessarily result in an increase in the lubricant's motion velocity. 3.4 Radial Distribution Functions.

The radial distribution function (RDF) is exclusively applicable to valid trajectories derived from molecular dynamics simulations. Its primary purpose is to characterize molecular structures. RDF serves as a probability function for determining the likelihood of encountering a pair of atoms at a given distance (r) relative to another atom within a randomly distributed atomic system.

In Figure 6, which depicts different shear velocities in various regions of a turbine, is observed that the curves for different shear velocities overlap. This indicates that change in shear velocity do not alter the bonds formed within the lubricant. Thus, it is evident that different mechanical demands on the lubricant do not impact it within the analyzed time of 400 ps.

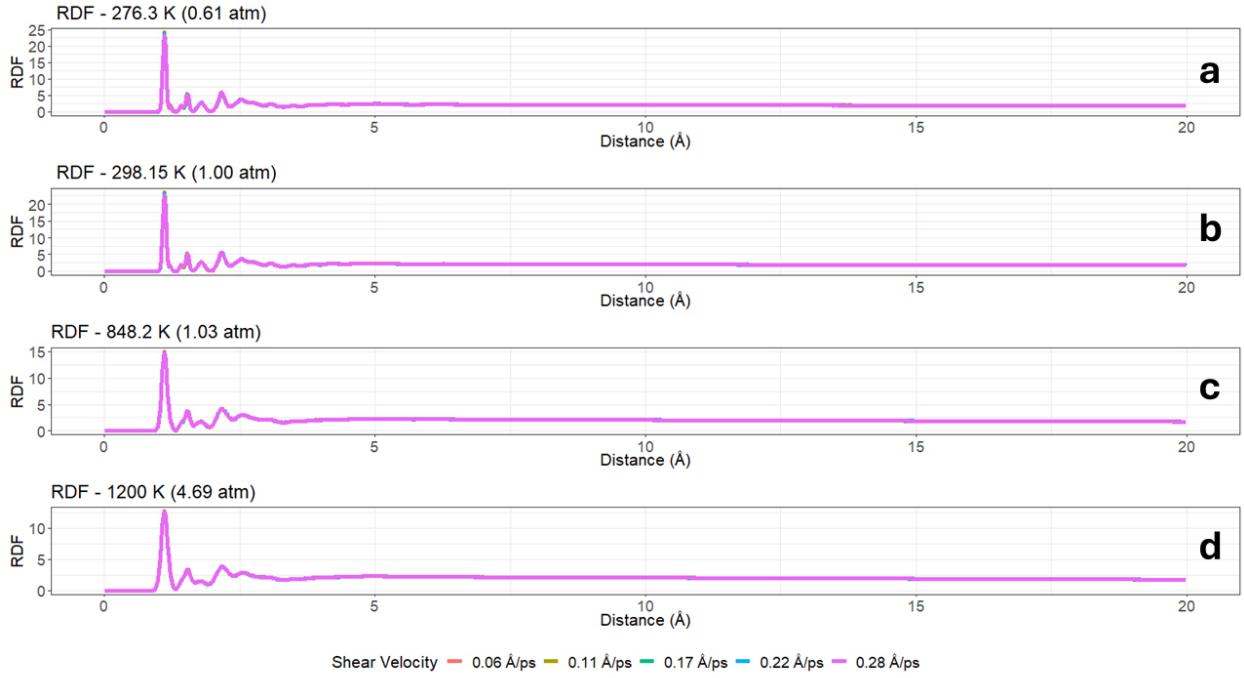

Figure 6. Curves illustrating radial distribution function under varying shear velocities in different settings: (a) Intake, (b) Ambient Conditions, (c) Outlet Nozzle, and (d) Combustion Chamber.

However, it should be noted that changes in the environment, particularly in pressure and temperature, impact the chemical structure of the lubricant. This is evident from the changes in the intensity of the presented peaks, which decrease with increasing pressure and temperature. This decrease indicates that in the turbine inlet region, the metal is surrounded by a greater amount of lubricant than in the combustion chamber and the turbine outlet region. In other words, at high pressures and temperatures, the outer layers of the lubricant start to interact more with the inner layers, providing fewer molecules to interact with the metal. It is likely that the high ambient pressure causes the molecules to become closer, leading to new Van der Waals interactions between the molecules. This behavior is reinforced by the friction coefficient results discussed earlier (Zhang et al. 2020, Li et al. 2016).

Mean Square Displacement

The Mean Square Displacement (MSD) technique is a highly effective method for describing the velocity and displacement of individual atoms within molecular chains in a model. In Figure 7, it is observed that all the curves show increases over time. Additionally, a pattern emerges where higher applied shear velocities correspond to higher MSD values, indicating greater the mobility of the lubricant molecules. The results presented in curves (A) and (B) are nearly identical because the pressure and temperature conditions are very similar. In the more extreme cases of temperature and pressure, represented by curves (C) and (D), there is a noticeable decrease in mobility compared to ambient conditions. This likely occurs because the pressure outweighs the kinetic energy gained from the ambient temperature, causing molecules to have lower mobility due to the applied force and increased chemical interaction within the lubricant itself, as indicated by the RDF results.

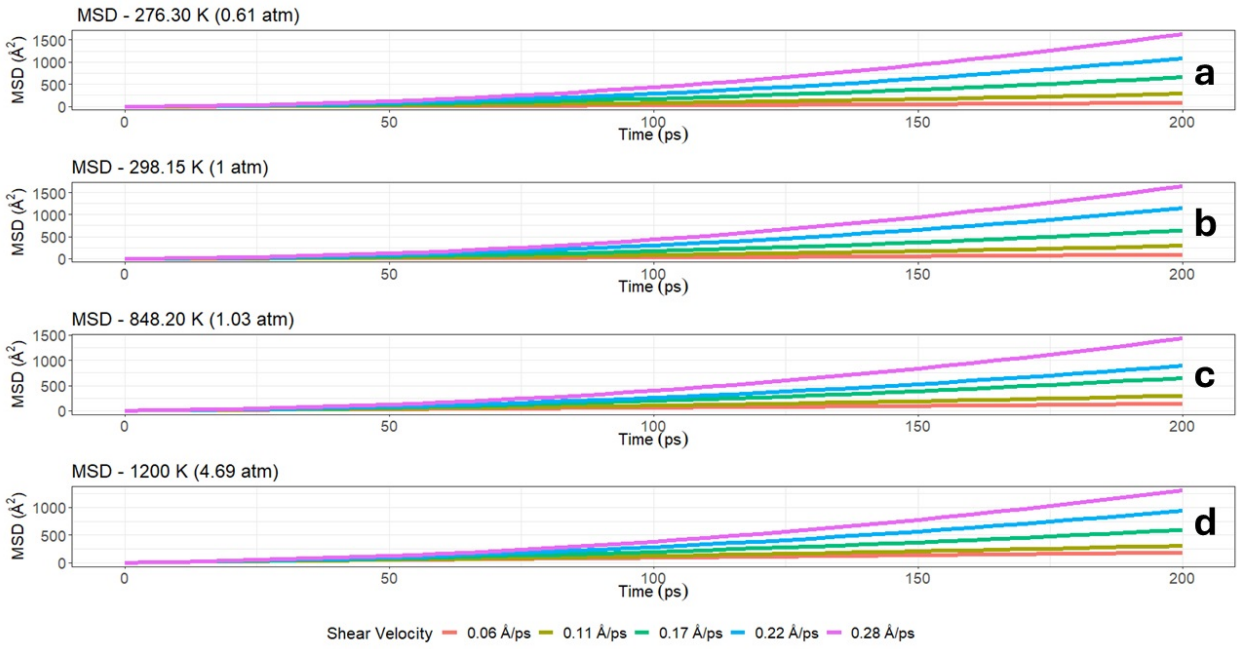

Figure 7. Curves illustrating mean square displacement under varying shear velocities in different settings: (a) Intake, (b) Ambient Conditions, (c) Outlet Nozzle, and (d) Combustion Chamber.

Friction Coefficient

After the shear process, the friction coefficient between nickel aluminide and Trimethylolpropanetriheptanoate ester was calculated using Equation (3).

$$l = \frac{FN}{FT}. \tag{3}$$

where l is defined as friction coefficient; and FN and FT are the normal force and friction force, respectively (Chawla & Sharma 2018). The results are shown in Figure 8. The curve illustrates the relationship between the friction coefficient and the shear velocity under the four distinct temperature and pressure conditions examined.

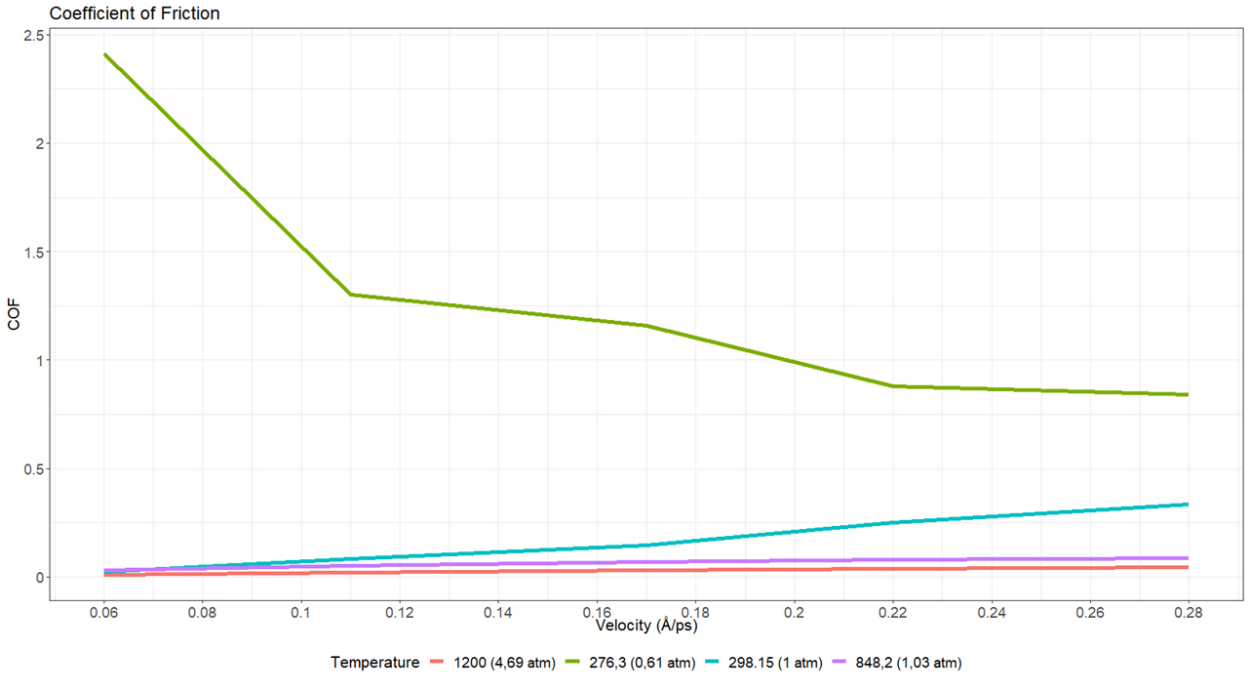

Figure 8. Friction coefficient of lubricant at different environmental conditions.

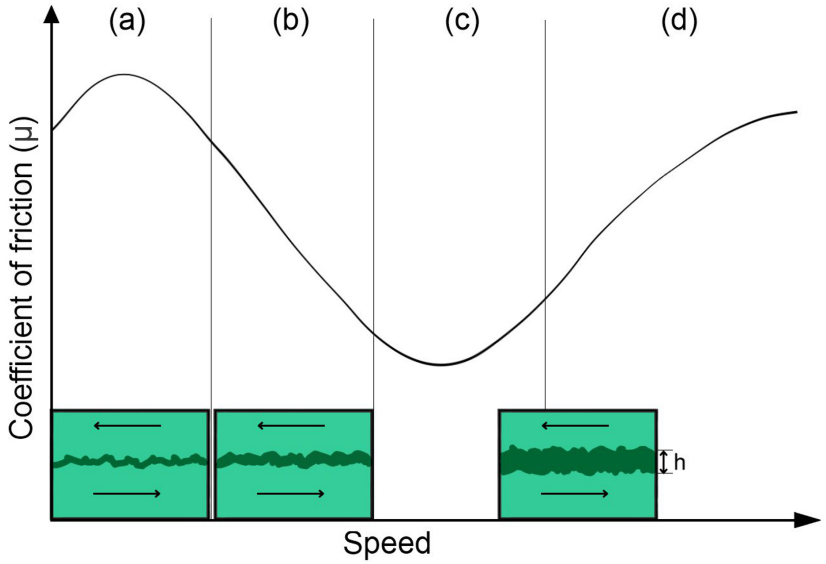

Figure 9. Stribeck curve: (a) the boundary regime; (b) the mixed regime; (c) the elasto-hydrodynamic regime; (d) the hydrodynamic regime

The sliding velocity in a lubrication system significantly affects its tribological behavior and the resulting coefficient of friction, typically illustrated using a a Stribeck curve (Figure 9) (Zhao et al. 2021). This curve can be segmented into four distinct lubrication regions, as described below:

- Mixed lubrication state (b): as the velocity increases, the lubricating oil generates fluid dynamic pressure. This pressure formation occurs within the fluid reduces direct contact between the two surfaces;
- Elastohydrodynamic lubrication state (c): friction is minimized when the surfaces are no longer in direct contact;
- Hydrodynamic lubrication zone (d): friction is predominantly influenced by the viscous resistance of the lubricant during rapid sliding. In this zone, the overall friction of the system increases due to the heightened internal friction of the lubricant.

The shear rate is a crucial factor in the tribological behavior of lubricants. Generally, an increase in shear rate can result in a reduction in the friction coefficient, facilitating the formation of a more effective lubricant layer between contacting surfaces. However, for non-Newtonian lubricants, such as viscoelastic or pseudoplastic ones, the behavior may be more complex. In these cases, the lubricant viscosity may decrease with increasing shear rate, potentially increasing friction and wear. Thus, shear rate directly influences the friction, wear, and lubricating capacity of lubricants on contacting surfaces.

In this study, it is observed that the rheological behavior of the lubricant changes with shear rate depending on the environment. At room temperature and pressure, the lubricant operates in the hydrodynamic zone; thus, an increase in shear rate leads to an increase in the internal friction of the lubricant, and consequently, an increase in the Coefficient of Friction (COF). When the pressure and temperature decrease, an increase in shear rate generates dynamic fluid pressure, reducing contact between surfaces and facilitating sliding in the system. Conversely, higher temperatures and pressures have little effect on the system's response to an increase in shear rate. However, a slight increase in COF is observed, indicating that the lubricant behaves as if it were in the hydrodynamic zone.

These observations highlight the lubricant's ability to alter its rheological behavior depending on environmental conditions. Specifically, it behaves as a Newtonian fluid under low temperatures and pressures (276.3 K - 0.61 atm) and as a non-Newtonian fluid under ambient conditions and at high temperatures. Therefore, under more extreme engine conditions, with high temperature and pressure, the lubricant will perform better under less intense mechanical demands, whereas the opposite is true under low temperature and pressure.

The highest friction coefficient (2.5 - 0.75) were observed at the lowest temperature and pressure evaluated, specifically 276.3 K and 61.95 kPa. In other parts of the turbine, the friction coefficient exhibited lower values (0 to 0.01), even smaller than under ambient conditions. This change in behavior is likely attributed to the combined effect of temperature and pressure on the internal configuration of the lubricant's chains. Typically, reduced adsorption at high temperatures and pressures compromises wear protection by diminishing boundary lubrication, thinning the lubricant film, promoting oxidation and degradation, and enhancing boundary friction. These factors underscore the importance of selecting suitable lubricants and designing systems to endure extreme operating conditions while ensuring optimal wear protection and equipment reliability. In such cases, the

lubricant may undergo chemical reactions or structural changes, resulting in a more robust protective film on the contacting surfaces. This enhanced film formation could lead to lower friction coefficients despite the reduction in adsorption of lubricant molecules. Additionally, under certain extreme conditions, the lubricant may exhibit non-Newtonian behavior, where its viscosity and flow properties change significantly. This altered behavior could potentially enhance lubricant performance and reduce friction under specific operating conditions.

Viscosity

To validate our viscosity calculations, we analyze the Self-Auto Correlation Function (SACF). This equilibrium molecular dynamics (EMD) technique examines the temporal fluctuations in stress tensors, relating them to viscosity via the Green-Kubo formula or Einstein relation (Lin & Kedzierski 2020). In this research, we used the Green-Kubo formula (equation 4). Initially, the SACF displays higher oscillations, gradually diminishing in amplitude, indicating the system's progression towards equilibrium from a non-equilibrium state. Furthermore, we examined the viscosity of the lubricant under environment condition (298.15 K – 0.000101325 GPa) and compared our simulation results with experimental data (Ross & Yaakov 1982). Remarkably, our MD simulation closely matched the experimental findings, validating the accuracy of our approach. The viscosity value obtained from the simulation was 4.85 x 104 cP, which is close to the experimental value of 0.2450 x 104 cP. To better visualize the difference between the values, the mean squared error was calculated, yielding a value of 21.23, an acceptable value for the simulation conducted. The slight discrepancy is likely due to the high viscosity of the lubricant, which requires extended simulation times that may exceed the relaxation time of the molecules (Lin & Kedzierski 2020).

$$\eta = \frac{V}{KT} \int_0^\infty \langle P_{\alpha\beta}(t).P_{\alpha\beta}(0)\rangle dt. \tag{4}$$

Where: η is the thermal conductivity of the system; V is the volume of the system; k is the Boltzmann constant; T is the absolute temperature of the system; (P$\alpha\beta$) is the heat current density at time; $\langle\rangle$ denotes ensemble average.

CONCLUSION

Upon analyzing the obtained results, it is evident that employing molecular dynamics simulations, facilitated by the commercial software Materials Studio, has proven effective for the intended objective. Specifically, this approach has been instrumental in assessing lubricant performance under the rigorous conditions of aircraft turbine operations, characterized by high temperatures and pressures. Hence, it emerges as a valuable tool for supporting professionals in the realm of aeronautical lubricants. To validate our simulation, we compared the viscosity results with experimental data. The values obtained from the simulation were consistent with the experimental data, with only a slight difference. Although we observed an acceptable mean squared error, it is important to note that the high viscosity of the lubricant may have limited the accuracy of the simulation due to the required simulation time, which may exceed the relaxation time of the molecules.

The lubricant exhibits improved efficiency and performance as the temperature and pressure to which it is subjected increase, as indicated by the results. The findings demonstrated that as pressure and temperature increased, there was reduced mobility of the polymer chains and increased interaction within the lubricant. This resulted in a lower amount of lubricant adsorbed on the metal, as evidenced by the relative concentration results. Consequently, the tribological performance of the material was enhanced, with the molecules in contact with the metal experiencing higher velocity and temperature, reflected in the lower coefficients of friction under these extreme usage conditions.

Additionally, the shear velocity demonstrated an influence on the tribological behavior of the lubricant, as evidenced by the friction coefficient results. This impact is due to the temperature and the velocity that the molecules at the interface with the metal acquire as a result of the applied shear velocity.

Thus, it is evident that both the environment and the mechanical demand on the lubricant are factors that impact its tribological performance. However, the mechanisms of each factor are distinct. While the environment exerts chemical influence, altering the chemical interactions of the lubricant, shear velocity physically affects the lubricant, aiding friction reduction through the increase in velocity and temperature within the system.

Therefore, the results elucidated in this article offer promising insights into the effectiveness of this methodology in fostering the development of new initiatives. Consequently, for forthcoming research endeavors aimed at expanding upon the current study, there are intentions to investigate the impact of oxidation on the tribological properties of the lubricant, alongside evaluating any performance modifications arising from the incorporation of additives into its formulation.

Acknowledgments

This study was financed in part by the Coordenação de Aperfeiçoamento de Pessoal de Nivel Superior (CAPES) Finance Code 001.

REFERENCES

ALI I ET AL. 2019. Advances in carbon nanomaterials as lubricants modifiers. J Mol Liq 279: 251-266.

BAKAN E, MACK DE, MAUER G, VASSEN R, LAMON J & PADTURE NP. 2020. High-temperature materials for power generation in gas turbines. p. 3-62. Elsevier.

BASHEER A. 2020. Advances in the smart materials applications in the aerospace industries. Aircr Eng Aerosp Tec 92(7): 1027-1035. doi:10.1108/AEAT-02-2020-0040.

CHAWLA R & SHARMA S. 2018. A molecular dynamics study on efficient nanocomposite formation of styrene–butadiene rubber by incorporation of graphene. Graphene Technol 3: 25-33. doi:10.1007/s41127-018-0018-9.

CUI J, ZHAO J, WANG S, WANG Y & LI Y. 2021. Effects of carbon nanotubes functionalization on mechanical and tribological properties of nitrile rubber nanocomposites: Molecular dynamics simulations. Comp Mater Sci 196: 110556. doi:10.1016/j.commatsci.2021.110556.

DEKOULIS G (Ed). 2019. Aerospace Engineering. London: IntechOpen. doi:10.5772/intechopen.79206. URL https://www.intechopen.com/books/8613.

EL-MAGLY IA, NAGIB HK & MOKTAR WM. 2018. Cordial physico-chemical characteristics of some trimethylolpropane triesters as base synthetic lubricant for turbo-jet aircrafts. Egypt J Pet 27: 1123-1130. doi:10.1016/j.ejpe.2018.04.002.

EL-SAYED AF. 2017. Aircraft Propulsion and Gas Turbine Engines, Second Edition. Boca Raton, USA: Taylor & Francis. doi:10.1201/9781315156743.

EWEN JP, HEYES DM & DINI D. 2018. Advances in nonequilibrium molecular dynamics simulations of lubricants and additives. Friction 6: 349-386. doi:10.1007/s40544-018-0207-9.

GUO F, ZHANG J, CHEN Z, ZHANG M, PEI J & LI R. 2021. Study on Adhesion Property and Moisture Effect between SBS Modified Asphalt Binder and Aggregate Using Molecular Dynamics Simulation. Constr Build Mater 300: 124037. doi:10.1016/j.conbuildmat.2021.124037.

HAILE JM. 1992. Molecular Dynamics Simulation: Elementary Methods. Clemson, USA: J Wiley & Sons, Inc.

HU C, YOU G, LIU J, DU S, ZHAO X & WU S. 2021. Study on the mechanisms of the lubricating oil antioxidants: Experimental and molecular simulation. J Mol Liq 324: 115099. doi:10.1016/j.molliq.2020.115099.

HUANG JC. 2012. Evaluation of Tribological Behavior of Al-Co-Cr-Fe-Ni High Entropy Alloy Using Molecular Dynamics Simulation. Scanning 34: 325-331. doi:10.1002/sca.21006.

JAILLET L, ARTEMOVA S & REDON S. 2017. IM-UFF: Extending the universal force field for interactive molecular modeling. J Mol Graph Model 77: 350-362. doi:10.1016/j.jmgm.2017.08.023.

LI Y, WANG S, WANG Q & XING M. 2016. Molecular dynamics simulations of tribology properties of NBR (Nitrile-Butadiene Rubber)/carbon nanotube composites. Composites Part B: Engineering 97: 62-67. doi:10.1016/j.compositesb.2016.04.053.

LIN L & KEDZIERSKI MA. 2020. Density and viscosity of a polyol ester lubricant: Measurement and molecular dynamics simulation. International Journal of Refrigeration 118: 188-201. doi:10.1016/j.ijrefrig.2020.07.004.

LIU X, ZHOU X, KUANG F, ZUO H & HUANG J. 2021. Mechanical and Tribological Properties of Nitrile Rubber Reinforced by Nano-SiO2: Molecular Dynamics Simulation. Tribol Lett 69: 54. doi:10.1007/s11249-021-01427-9.

MEETHAM GW. 1981. The Development of Gas Turbine Materials. Essex, Michigan: Applied Science Publishers Ltd.

NAGENDRAMMA P & KAUL S. 2012. Development of Ecofriendly/Biodegradable Lubricants: An Overview. Renew Sustain Energy Rev 16: 764-774. doi:10.1016/j.rser.2011.09.002.

PAN L, YU H, LU S & LIN G. 2021. Effects of surface nanostructure on boundary lubrication using molecular dynamics. Nanotechnology and Precision Engineering 4: 033005. doi:10.1063/10.0005222.

PETRESCU RV, AVERSA R, AKASH B, BUCINELL R, CORCHADO J, BERTO F, MIRSAYAR M, APICELLA A & PETRESCU FIT. 2017. Modern Propulsions for Aerospace-A Review. J Aircr Spacecr Technol 1: 1-8. doi:10.3844/jastsp.2017.1.8.

QI Y, SUN B, ZHANG Y, GAO G, ZHANG P & ZHENG X. 2023. Tribological Properties of Nano-ZrO2 and PEEK Reinforced PTFE Composites Based on Molecular Dynamics. Lubricants 11: 194. doi:10.3390/lubricants11050194.

RAOF NA, YUNUS R, RASHID U, AZIS N & YAAKUB Z. 2019. Effect of molecular structure on oxidative degradation of ester-based transformer oil. Tribol Int 140: 105852. doi:10.1016/j.triboint.2019.105852.

RAPPE AK, CASEWIT CJ, COLWELL KS, GODDARD WA & SKIFF WM. 1992. UFF, a full periodic table force field for molecular mechanics and molecular dynamics simulations. J Am Chem Soc 114: 10024-10035. doi:10.1021/ja00051a040.

ROSS S & YAAKOV S. 1982. Lubricant Foaming and Aeration Study. Interim Technical Report AFWAL-TR-82-2090. Aero Propulsion Laboratory, Air Force Wright Aeronautical Laboratories. Wright-Patterson Air Force Base, Ohio, USA. URL https://apps.dtic.mil/sti/tr/pdf/ADA124184.pdf.

SIOURIS S, SHEPHERD T, WILSON C & BLAKEY S. 2013. Development of an Apparatus for the Degradation of Aviation Gas Turbine Lubricants. Tribol T 56: 215-223.

SIOURIS S & WILSON C. 2010. Thermodynamic Properties of Pentaerythritol-Based Species Involved in Degradation of Aviation Gas Turbine Lubricants. Ind Eng Chem Res 49: 12294-12301.

SRIVASTAVA I, KOTIA A, GHOSH SK & ALI MKA. 2021. Recent advances of molecular dynamics simulations in nanotribology. J Mol Liq 335: 116154.

SU M, SI C, ZHANG Z & ZHANG H. 2020. Molecular dynamics study on influence of Nano-ZnO/SBS on physical properties and molecular structure of asphalt binder. Fuel 263: 116777. doi:10.1016/j.fuel.2019.116777.

SUN J & DU S. 2019. Application of graphene derivatives and their nanocomposites in tribology and lubrication: a review. RSC Advances 9: 40642-40661.

TA DT, TIEU AK, ZHU H & KOSASIH B. 2015. Thin film lubrication of hexadecane confined by iron and iron oxide surfaces: A crucial role of surface structure. J Chem Phys 143: 164702.

TALAPATRA A & DATTA D. 2023. A review of the mechanical, thermal and tribological properties of graphene reinforced polymer nanocomposites: a molecular dynamics simulations methods. Polym Bull 80: 2299-2328.

WAKIRU JM, PINTELON L, MUCHIRI PN & CHEMWENO PK. 2019. A review on lubricant condition monitoring information analysis for maintenance decision support. Mech Syst Signal Pr 118: 108-132.

WU N, ZONG Z, FEI Y, MA J & GUO F. 2017. Thermal oxidation stability of poly-α-olefin lubricating oil. Asia-pac J Chem Eng 12: 813-817.

XU Q, ZHANG J, HU YZ & MA TB. 2021. Tribological Behavior of Poly(tetrafluoroethylene) and Its Composites Reinforced by Carbon Nanotubes and Graphene Sheets: Molecular Dynamics Simulation. Physica Status Solidi (RRL) – Rapid Research Letters 16: 1-8.

YIN Y, SONG J, ZHAO G & DING Q. 2022. Improving the high temperature tribology of polyimide by molecular structure design and grafting POSS. Polymer Advanced Technologies 33: 886-896.

ZENG Q & CHEN T. 2018. Superlow friction and oxidation analysis of hydrogenated amorphous silicon films under high temperature. J Non-cryst Solids 493: 73-81.

ZHANG T, HUANG H, LI W, CHANG X, CAO J & HUA L. 2020. A molecular dynamics study of lubricating mechanism of graphene nanoflakes embedded in Cu-based nanocomposite. Tribol Lett 68: 1-11.

ZHAO P, DONG M, YANG Y, SHI J, WANG J, WU W, ZHAO X, ZHOU X & WANG C. 2021. Research on the Mechanism of Surfactant Warm Mix Asphalt Additive-Based on Molecular Dynamics Simulation. Coatings 11: 1303.

ZOJAJI M, HYDARINASAB A, HASHEMABADI SH & MEHRANPOUR M. 2021. Rheological behaviour of shear thickening fluid of graphene oxide and SiO2 polyethylene glycol 400-based fluid with molecular dynamic simulation. Mol Simulat 1-9.

How to cite
SOUZA CB, GONÇALVES RFB & ROCCO JAFF. 2024. Analysis of Tribology Properties of Trimethylolpropane-based Lubricant by Molecular Dynamics. An Acad Bras Cienc 96: e20240040. DOI 10.1590/0001-3765202420240040.

Manuscript received on January 28, 2024;
accepted for publication on June 17, 2024

CAMILA B. SOUZA
https://orcid.org/0000-0002-2444-4912

RENE FRANCISCO B. GONÇALVES
https://orcid.org/0000-0001-7731-3847

JOSÉ ATÍLIO F.F. ROCCO
https://orcid.org/0000-0002-6004-6997

Instituto Tecnológico da Aeronáutica, Praça Marechal Eduardo Gomes, 50, 12228-900 São José dos Campos, SP, Brazil

Correspondence to: **José Atílio F.F. Rocco**

E-mail: jose.fritz@gp.ita.br

Author contributions

The simulation part of the study, including data collection and subsequent analysis, was conducted by Camila B. Souza. The discussion and interpretation of the results were a collaborative effort between all the authors. Rene Francisco B. Gonçalves and José Atílio F. F. Rocco contributed significantly to the development of the theoretical framework underlying the research.